Inclusive distributions for hadronic collisions in the valon-recombination model

Rudolph C. Hwa[1] and C. B. Yang[1,2]
[1]*Institute of Theoretical Science and Department of Physics, University of Oregon, Eugene, Oregon 97403-5203*
[2]*Institute of Particle Physics, Hua-Zhong Normal University, Wuhan 430079, People's Republic of China*
(Received 22 April 2002; published 27 August 2002)

Inclusive distributions of soft production of mesons in hadronic collisions are calculated in the valon-recombination model. The new determination of the valon distributions from hard scattering data makes possible a tightly interrelated treatment of pion and kaon production in the fragmentation regions of proton, pion, and kaon. Only one free parameter is used in the determination of the valon distribution in the kaon. No other adjustable parameter is needed to fit the x distributions of the data on inclusive cross sections, except for the normalizations since the data are at fixed p_T. The success of the model in reproducing seven inclusive distributions suggests that there are two important mechanisms at work in soft production. One is that the structure of the hadron that fragments is highly relevant. The other is that the produced particles are formed by the recombination of quarks and antiquarks. These two aspects about hadrons in soft processes can be well described in the framework of the valon-recombination model.

DOI: 10.1103/PhysRevC.66.025205 PACS number(s): 13.85.Ni, 13.85.Hd, 25.80.Hp

I. INTRODUCTION

Particle production at low p_T in hadronic collisions has always been a challenge for theoretical models to describe, since, on the one hand, it is a process that is nonperturbative, while, on the other hand, meaningful modeling can only be done in the framework of quarks and gluons. The subject has a long history, some early reviews of which can be found in Refs. [1,2]. Since soft processes, as they are called, cannot be treated by perturbative QCD, they have not been given the degree of rigorous scrutiny that has been accorded hard processes. Among the models that are constructed for soft processes, there are basically only two types: string models that make use of fragmentation [3,4] and parton models that are based on recombination [5,6]. This paper treats the modernization of the latter. What is new is that the parton distributions of the proton have recently been calculated by CTEQ in pQCD over wide ranges of x and Q^2, fitting a large collection of experimental data [7]. From such parton distributions the structure of the proton in terms of the valons [8] can be more precisely determined [9]. With the new parametrization of the valon model now available, it is possible to revisit the problem of hadron production in soft processes and calculate the inclusive distributions of the produced particles without adjustable parameters. Good agreement with the low-p_T experimental data can give definitive support to the recombination model.

The kinematical region in which we focus our attention is the projectile fragmentation region, roughly $x>0.2$. In the central region the structure of the projectile hadron is less important. But in the fragmentation region it is known as early as the mid-1970s that the inclusive distribution of the produced pions is closely related to the structure function of the proton, as observed by Ochs [10]. The recombination model [5] is a realization of that observation, and the valon model is a self-consistent formulation of the unification of hadron structure and recombination probability [6]. In short, our view is that, while the fragmentation of strings may be suitable for the central region, the recombination of partons is more relevant for the fragmentation region.

It has been regarded as a striking confirmation of the dual parton model (DPM) [3] to reproduce the charge distribution of the produced particles in $\pi^+ p$ collisions; the forward-backward asymmetry [11] is presented as evidence for the two-chain diquark fragmentation of the proton. While the qualitative agreement with data gives support to the two-chain mechanism of DPM as opposed to the single-chain mechanism of the Lund model, the data (not cited in Ref. [3]) were old and inaccurate and the theoretical calculations were crude. The data that we shall compare with are detailed and more precise [12]. Moreover, we shall consider a large number of fragmentation processes: $p\to\pi^\pm$, $\pi^\pm\to\pi^\mp$, $K^+\to\pi^\pm$, and $\pi^+\to K^\pm$, and the results of our calculations can all be compared with existing data. To our knowledge such data have never been used before to confront model calculations. That the valon-recombination model is able to reproduce those data, as we shall show in this paper, should therefore be regarded as meeting a higher demand than fitting the charge asymmetry of $\pi^+ p$ collisions discussed in Ref. [3].

Another reason for revisiting the soft processes in hadronic collisions is that the recent development in heavy-ion collisions at high energies presents some urgency to understand better the basic processes of particle production at a more fundamental level. To understand the formation of dense matter, it is necessary to understand first baryon stopping and pionization in pA collisions. We have recently done a comprehensive treatment of the problem of momentum degradation in pA collisions in the framework of the valon model [13]. The emphasis is on the nuclear effects on the projectile. The parameters used for the valon and parton distribution functions have not been put to test on the hadronic collisions. Since those distributions have been updated even more recently [9], it is necessary to focus on the elementary processes, not only of pp, but also of meson-proton collisions, in order to check the valon-recombination model (VRM) to a degree never attempted before. It is toward that end that we apply the VRM to the soft processes in this paper.

II. VALON AND PARTON DISTRIBUTION FUNCTIONS

The valon model describes the hadron structure relevant for multiparticle production. The momentum distributions of the valons can be determined from the parton distributions at low Q^2, as posted by CTEQ4LQ [14]. That was done very recently [9], resulting in excellent fits of the u and d quark distributions. The parameters describing the valon distributions turn out to be quite different from the old values based on imprecise muon and neutrino data of the 1970s [8], although the formalism of the model remains the same. Furthermore, the assumption of the symmetric sea used previously has been lifted so that the parton distributions in the valons are now also very different. Here we give a summary of the valon and parton distributions functions, the details of which can be found in Ref. [9].

In a proton the three-valon distribution is

$$G_{UUD}(y_1,y_2,y_3)=g_p(y_1y_2)^\alpha y_3^\beta \delta(y_1+y_2+y_3-1), \quad (1)$$

where y_i is the momentum fraction of the ith valon (y being never used for rapidity in this paper), and

$$g_p=[B(\alpha+1,\beta+1)B(\alpha+1,\alpha+\beta+2)]^{-1}, \quad (2)$$

$B(m,n)$ being the beta function. The single valon distributions are obtained by integration

$$G_U(y)=\int dy_2 \int dy_3 G_{UUD}(y,y_2,y_3) = g_p B(\alpha+1,\beta+1) y^\alpha (1-y)^{\alpha+\beta+1}, \quad (3)$$

$$G_D(y)=\int dy_1 \int dy_2 G_{UUD}(y_1,y_2,y) = g_p B(\alpha+1,\alpha+1) y^\beta (1-y)^{2\alpha+1}. \quad (4)$$

The new values of α and β are found to be [9]

$$\alpha=1.76 \quad \text{and} \quad \beta=1.05, \quad (5)$$

which are significantly different from those used in Refs. [6,13] due to various theoretical assumptions and limited experimental data.

Since each valon contains one and only one valence quark of its own flavor, the valence quark distributions are convolutions of the relevant valon distributions with the valence (nonsinglet) quark distributions in the valons. In terms of moments we have simple products

$$\tilde{u}_v(n)=2\tilde{G}_U(n)\tilde{K}_{NS}(n), \quad (6)$$

$$\tilde{d}_v(n)=\tilde{G}_D(n)\tilde{K}_{NS}(n), \quad (7)$$

where

$$\tilde{G}_{U,D}(n)=\int_0^1 dy y^{n-1} G_{U,D}(y), \quad (8)$$

and similarly for $\tilde{q}_v(n)$ in terms of $q_v(x)$ where q stands for either u or d. The value of Q^2 is set at $1(\mathrm{GeV}/c)^2$ for application of the model to low-p_T processes and will not be exhibited explicitly. From Eqs. (3) and (4) we have

$$\tilde{G}_U(n)=B(\alpha+n,\alpha+\beta+2)/B(\alpha+1,\alpha+\beta+2), \quad (9)$$

$$\tilde{G}_D(n)=B(\beta+n,2\alpha+2)/B(\beta+1,2\alpha+2). \quad (10)$$

The n dependence of $\tilde{K}_{NS}(n)$ is determined in Ref. [9] and fitted by the following parametrization:

$$\tilde{K}_{NS}(n)=\exp\left(-\sum_{j=0}^{3} c_j u^j\right), \quad u=\ln(n-1), \quad (11)$$

where $c_j=0.753$, 0.401, 0.0962, and 0.0555, for $j=0$, 1, 2, 3, respectively.

For the sea quark distributions in the valons we have found that the SU(2) symmetry has to be broken to fit the CTEQ4 data, and that the favored quark distributions (u in U and d in D) are suppressed relative to the unfavored quark distributions (u in D and d in U), consistent with Pauli blocking. They are denoted, respectively, by $L_f(z)$ and $L_u(z)$, which are different from the s-quark distribution $L_s(z)$ and the gluon distribution $L_g(z)$. The distributions of these partons in the proton are given, in terms of the moments, simply by sums of products

$$\tilde{\bar{u}}=2\tilde{G}_U\tilde{L}_f+\tilde{G}_D\tilde{L}_u, \quad (12)$$

$$\tilde{\bar{d}}=\tilde{G}_D\tilde{L}_f+2\tilde{G}_U\tilde{L}_u, \quad (13)$$

$$\tilde{s}=(2\tilde{G}_U+\tilde{G}_D)\tilde{L}_s, \quad (14)$$

$$\tilde{g}=(2\tilde{G}_U+\tilde{G}_D)\tilde{L}_g, \quad (15)$$

where the dependences on n have been omitted. The functions $\tilde{L}_i(n)$ are parametrized as follows [9]:

$$\ln\tilde{L}_i(n)=-\sum_{j=0}^{3} b_j^{(i)} u^j, \quad u=\ln(n-1), \quad (16)$$

where $b_j^{(i)}$ are given in Table I.

TABLE I. Coefficients in Eq. (16).

i	$b_0^{(i)}$	$b_1^{(i)}$	$b_2^{(i)}$	$b_3^{(i)}$
f	4.12	2.2	0.2	0.18
u	3.07	1.5	0.08	0.05
s	4.21	1.6	0.1	0.02
g	0.98	1.0	0.05	0

For meson-initiated reactions we need the valon distributions in mesons, which can be determined from the quark distributions in mesons on the basis of the universality of the quark distributions in valons. From experimental data on Drell-Yan and prompt photon production in $\pi^\pm N$ collisions, the parton distributions in the pion have been determined in Ref. [15], using the parametrization

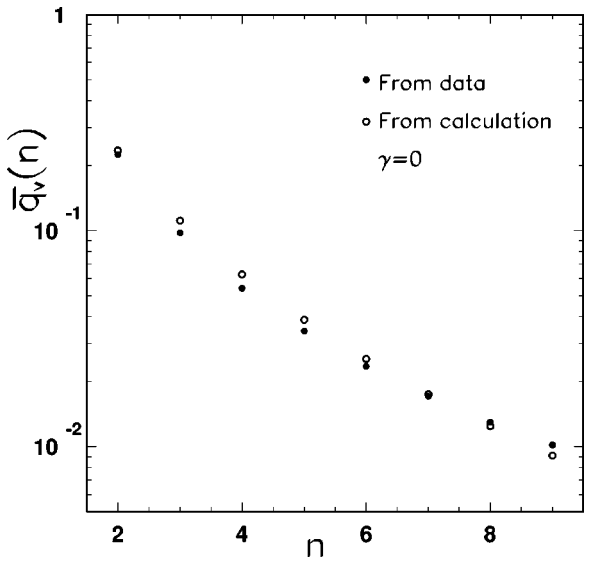

FIG. 1. Moments of the valence quark distribution in a pion, $\tilde{q}_v(n)$, where the parameter γ is chosen to fit the moments of distribution determined from the experimental data [15].

$$xq_v(x)=A_v x^{\alpha'}(1-x)^{\beta'} \tag{17}$$

for the valence quarks with $\alpha'=0.64\pm0.03$ and $\beta'=1.11\pm0.04$. In the valon model for the pion that distribution is related to the valon distribution by

$$xq_v(x)=\int_0^1 dy_1\int_0^{1-y_1} dy_2 G^{\pi}(y_1,y_2)K_{NS}(x/y_1), \tag{18}$$

where $K_{NS}(z)$ is identified with the same in the proton problem. Since the two valons in pion are symmetrical, we use the valon distribution

$$G^{\pi}(y_1,y_2)=g_{\pi}(y_1y_2)^{\gamma}\delta(y_1+y_2-1), \tag{19}$$

where $g_{\pi}=1/B(\gamma+1,\gamma+1)$. We convert Eq. (18) to the moment form

$$\tilde{q}_v(n)=\tilde{G}^{\pi}(n)\,\tilde{K}_{NS}(n), \tag{20}$$

where $\tilde{G}^{\pi}(n)$ involves only one parameter γ, and $\tilde{K}_{NS}(n)$ is the same as in Eq. (11) on the basis of the universality of the valon structure, independent of the host hadron. The corresponding moment of Eq. (17) can trivially be calculated. Both are shown in Fig. 1, where a good agreement between the two is achieved by the choice

$$\gamma=0. \tag{21}$$

This value is also consistent with the one used in Ref. [6]. Thus $g_{\pi}=1$, and the single valon distribution in a pion is simply

$$G^{\pi}(y)=1. \tag{22}$$

The flat distribution of the valons in pion is a result of the fact that the constituent quarks are much more massive than the pion so they are tightly bound, resulting in large uncertainty in the valon momentum fraction.

The situation with the K meson is somewhat different, since the kaon mass is higher, and the constituent quarks have unequal masses. The valon distribution has a form similar to that of the pion in Eq. (19),

$$G^K(y_1,y_2)=g_K y_1^a y_2^b \delta(y_1+y_2-1), \tag{23}$$

where $g_K=1/B(a+1,b+1)$. The average momentum fractions of the two valons are

$$\overline{y}_{1,2}=\int dy_1 dy_2 y_{1,2} G^K(y_1,y_2) \tag{24}$$

so their ratio is

$$\overline{y}_1/\overline{y}_2=(a+1)/(b+1). \tag{25}$$

Since the average velocities of the two valons are the same as that of the host kaon, their momenta should be proportional to their masses, i.e., $\overline{y}_1/\overline{y}_2\approx m_U/m_S$. Taking the constituent quark masses of u and s types to be in the ratio 2:3, we get from Eq. (25)

$$b=(3a+1)/2. \tag{26}$$

Thus we are left with one unknown parameter in Eq. (23). Since the parton distributions in kaon are not known, we cannot determine that parameter as in the pion case. It will, however, be determined by the soft production data of kaon-initiated collisions later in Sec. V.

Knowing the valon distributions in mesons results in our knowledge of the recombination functions for the formation of the same mesons. Since we define the recombination function in the invariant phase space, we have from Eqs. (19) and (23)

$$R_{\pi}(x_1,x_2,x)=\frac{x_1x_2}{x^2}\,\delta\left(\frac{x_1}{x}+\frac{x_2}{x}-1\right), \tag{27}$$

$$R_K(x_1,x_2,x)=g_K\left(\frac{x_1}{x}\right)^{a+1}\left(\frac{x_2}{x}\right)^{b+1}\delta\left(\frac{x_1}{x}+\frac{x_2}{x}-1\right) \tag{28}$$

with a and b being constrained by Eq. (26). In this paper we do not consider nucleon production, so R_p is not needed (see Ref. [13]).

III. PROTON FRAGMENTATION

In a pp collision the soft production process in the fragmentation region is treated in the VRM as one in which the proton bag is broken by the collision and the valons become clusters of partons. The central idea of the model is that the probability for detecting a meson at large x is higher for a q

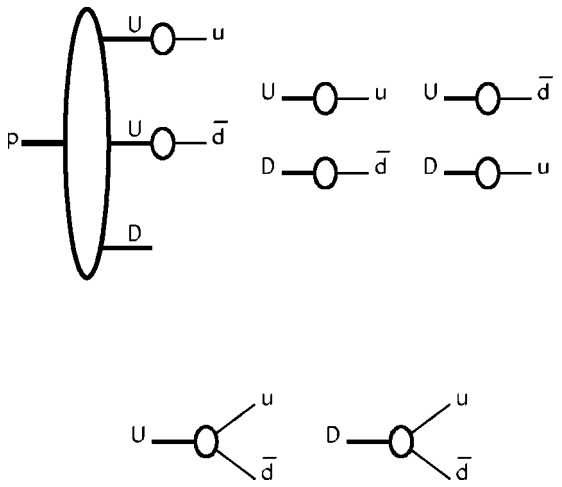

FIG. 2. Schematic diagrams in the VRM for the production of π^+ and π^- in the proton fragmentation region; only the $u\bar{d}$ and $d\bar{u}$ states are shown.

and a $\bar{q}$ at lower x_i to recombine than for a q or a diquark at high x' to fragment. The distributions of $q(x_1)$ and $\bar{q}(x_2)$ depend on the hadron structure. Under the assumption that the collision process does not significantly perturb the parton distributions outside the central interaction region (i.e., $x_i \geqslant 0.1$), the valon model can provide a sensible link between hadron structure and parton distributions. Since glueballs have never been seen, the gluons hadronize by first converting to $q\bar{q}$ pairs, thereby enhancing the sea. Downstream the quarks and antiquarks dress themselves and become the valons to be recombined in forming the produced particles. Since the dressing process does not change the total momentum of a quark, the meson momentum x is simply the sum of x_1 and x_2 of the q and $\bar{q}$, and the probability of hadronization is determined by an integration of the enhanced $q(x_1)$ and $\bar{q}(x_2)$ weighted by the recombination function. This is an s-channel description of the fragmentation process, the initial formulation of which is given in Ref. [6]. What we have now are the new distributions [9] and the more extensive low-p_T data [12] not available to be considered in Ref. [6].

Quantitatively, the invariant distribution for pion production in the proton fragmentation region is

$$x\frac{dN_\pi}{dx} = H_\pi(x) = \int \frac{dx_1}{x_1}\frac{dx_2}{x_2} F_\pi(x_1,x_2) R_\pi(x_1,x_2,x), \tag{29}$$

where $F_\pi(x_1,x_2)$ is the invariant distribution for q at x_1 and $\bar{q}$ at x_2, and is a convolution of the valon distribution in a proton with the quark distributions in valons, whose sea quarks are enhanced. In Fig. 2 we show the subprocesses giving u and $\bar{d}$ quarks by schematic diagrams, which represent

$$\begin{aligned} F_{\pi^+}(x_1,x_2) = \int dy_1 dy_2 [& G_{UU}(y_1,y_2) K(x_1/y_1) L'_u(x_2/y_2) \\ & + 2G_{UD}(y_1,y_2) K(x_1/y_1) L'_u(x_2/y_2) \\ & + 2G_{UD}(y_1,y_2) L'_u(x_1/y_1) L'_u(x_2/y_2)] \\ & + \int dy \left[2G_U(y) \left\{ K\left(\frac{x_1}{y}\right) L'_u\left(\frac{x_2}{y-x_1}\right) \right\}_{12} \right. \\ & \left. + G_D(y) \left\{ L'_u\left(\frac{x_1}{y}\right) L'_u\left(\frac{x_2}{y-x_1}\right) \right\}_{12} \right], \end{aligned} \tag{30}$$

where

$$K(z) = K_{NS}(z) + L'_f(z). \tag{31}$$

$L'_f(z)$ and $L'_u(z)$ are favored and unfavored sea quark distributions in a valon, enhanced by gluon conversion, and will be discussed below. In Eq. (30) the symbol $\{\cdots\}_{12}$ implies symmetrization in x_1 and x_2. Equation (30) can appear simpler in moment form, for which we define

$$\tilde{F}_{\pi^+}(n_1,n_2) = \int_0^1 dx_1 \int_0^{1-x_1} dx_2 x_1^{n_1-2} x_2^{n_2-2} F_{\pi^+}(x_1,x_2), \tag{32}$$

so that Eq. (30) becomes

$$\begin{aligned} \tilde{F}_{\pi^+}(n_1,n_2) = & [\tilde{G}_{UU}(n_1,n_2) + .2\tilde{G}_{UD}(n_1,n_2)] \tilde{K}(n_1) \tilde{L}'_u(n_2) \\ & + 2\tilde{G}_{UD}(n_1,n_2) \tilde{L}'_u(n_1) \tilde{L}'_u(n_2) + 2\tilde{G}_U(n_1+n_2 \\ & - 1) \{\tilde{K}(n_1,n_2) \tilde{L}'_u(n_2)\}_{12} + \tilde{G}_D(n_1+n_2-1) \\ & \times \{\tilde{L}'_u(n_1,n_2) \tilde{L}'_u(n_2)\}_{12}, \end{aligned} \tag{33}$$

where

$$\tilde{K}(n_1,n_2) = \int_0^1 dz z^{n_1-2} (1-z)^{n_2-1} K(z) \tag{34}$$

and similarly for $\tilde{L}'_u(n_1,n_2)$. For π^- we have

$$\begin{aligned} \tilde{F}_{\pi^-}(n_1,n_2) = & [\tilde{G}_{UU}(n_1,n_2) + 2\tilde{G}_{UD}(n_1,n_2)] \tilde{L}'_u(n_1) \tilde{L}'_u(n_2) \\ & + 2\tilde{G}_{UD}(n_1,n_2) \tilde{L}'_u(n_1) \tilde{K}(n_2) + 2\tilde{G}_U(n_1+n_2 \\ & - 1) \{\tilde{L}'_u(n_1,n_2) \tilde{L}'_u(n_2)\}_{12} + \tilde{G}_D(n_1+n_2-1) \\ & \times \{\tilde{K}(n_1,n_2) \tilde{L}'_u(n_2)\}_{12}. \end{aligned} \tag{35}$$

To use these in Eq. (29) we note that the moments of $H'_\pi(x) = x^3 H_\pi(x)$ is, using Eq. (27),

$$\tilde{H}'_\pi(n)=\int_0^1 dx x^{n-2}H'_\pi(x)$$
$$=\int_0^1 dx_1\int_0^{1-x_1}dx_2 F_\pi(x_1,x_2)(x_1+x_2)^n$$
$$=\sum_{[n_i]}\frac{n!}{n_1!n_2!}\tilde{F}_\pi(n_1+2,n_2+2), \quad (36)$$

where the sum over n_1 and n_2 is restricted by the constraint $n_1+n_2=n$. The double moments of the two-valon distributions are

$$\tilde{G}_{UU}(n_1,n_2)$$
$$=\int dy_1 dy_2 y_1^{n_1-1}y_2^{n_2-1}G_{UUD}(y_1,y_2,y_3)$$
$$=g_p\int_0^1 dy_1\int_0^{1-y_1}dy_2 y_1^{n_1+\alpha-1}y_2^{n_2+\alpha-1}(1-y_1-y_2)^\beta$$
$$=g_p B(n_1+\alpha,n_2+\alpha+\beta+1)B(n_2+\alpha,\beta+1), \quad (37)$$

$$\tilde{G}_{UD}(n_1,n_2)=\int dy_1 dy_3 y_1^{n_1-1}y_3^{n_2-1}G_{UUD}(y_1,y_2,y_3)$$
$$=g_p B(n_1+\alpha,n_2+\alpha+\beta+1)B(n_2+\beta,\alpha+1), \quad (38)$$

where g_p is given by Eq. (2).

For the enhanced sea quark distributions, $L'_f(z)$ and $L'_u(z)$, we recall that the quiescent sea as probed by electroweak interaction is described by $L_f(z)$ and $L_u(z)$, given in Ref. [9]. For either a U or D valon, the momentum fractions of all its partons add up to 1, so we have a constraint on the $n=2$ moments,

$$\tilde{K}_{NS}(2)+2[\tilde{L}_f(2)+\tilde{L}_u(2)]+2\tilde{L}_s(2)+\tilde{L}_g(2)=1. \quad (39)$$

The various terms above correspond to (for U valon, say) u valence, $u\bar{u}$ sea, $d\bar{d}$ sea, $s\bar{s}$ sea, and gluons. For hadronization we consider the enhanced sea where the gluons are completely converted into the $u\bar{u}$ and $d\bar{d}$ sectors, a scenario which we refer to as the saturated sea. Note that we do not let the gluons be converted to the $s\bar{s}$ sector due to the higher s-quark mass. Such a restriction should be relaxed in the case of nuclear collisions because of substantial Pauli blocking in the nonstrange sectors. Thus we write

$$\tilde{K}_{NS}(2)+2[\tilde{L}'_f(2)+\tilde{L}'_u(2)]+2\tilde{L}_s(2)=1. \quad (40)$$

From these two equations follows

$$\tilde{L}_g(2)=2[\tilde{L}'_f(2)+\tilde{L}'_u(2)-\tilde{L}_f(2)-\tilde{L}_u(2)]. \quad (41)$$

Assuming that the enhancement factor f_q is the same for favored and unfavored quarks, i.e., $\tilde{L}'_{f,u}(2)=f_q\tilde{L}_{f,u}(2)$, we get

$$f_q=1+\frac{\tilde{L}_g(2)}{2[\tilde{L}_f(2)+\tilde{L}_u(2)]}. \quad (42)$$

From Table I, the values of $\ln\tilde{L}_i(2)$ are found to be -4.12, -3.07, and -0.98, for $i=f$, u, and g, respectively. One thus obtains

$$f_q=3.99. \quad (43)$$

We assume that this enhancement factor applies uniformly at all z so that we have

$$L'_{f,u}(z)=f_q L_{f,u}(z), \quad \text{or} \quad \tilde{L}'_{f,u}(n)=f_q\tilde{L}_{f,u}(n). \quad (44)$$

This assumption is made mainly for the sake of simplicity and to avoid introducing undetermined parameters. It cannot be expected to be valid at very low z where the density is high, but that is outside the region of applicability of VRM anyway.

The two last quantities in Eqs. (33) and (35) that remain to be specified are $\tilde{K}(n_1,n_2)$ and $\tilde{L}'_u(n_1,n_2)$. They both are defined by integrals of the type given in Eq. (34) in terms of $K_{NS}(z)$, $L'_f(z)$ and $L'_u(z)$, the latter two being proportional to $L_f(z)$ and $L_u(z)$. Since the single moments $\tilde{K}_{NS}(n)$, $\tilde{L}_f(n)$, and $\tilde{L}_u(n)$ are given in Eqs. (11) and (16), we consider a direct approach to calculating $\tilde{K}(n_1,n_2)$ and $\tilde{L}'_u(n_1,n_2)$. Denoting $K_{NS}(z)$, $L_f(z)$, and $L_u(z)$ collectively by $J(z)$, we determine the double moments

$$\tilde{J}(n_1,n_2)=\int_0^1 dz z^{n_1-2}(1-z)^{n_2-1}J(z) \quad (45)$$

by expanding $(1-z)^{n_2-1}$ in powers of z up to $O(z^{n_2})$, since $J(z)$ is small as $z\to 1$, and the binomial coefficient c_m decreases rapidly with m. Thus to a very good approximation we can write

$$\tilde{J}(n_1,n_2)=\sum_{m=0}^{n_2}(-1)^m\binom{n_2-1}{m}\tilde{J}(n_1+m), \quad (46)$$

from which we can calculate $\tilde{K}(n_1,n_2)$ and $\tilde{L}'_u(n_1,n_2)$.

Having specified all the terms in Eqs. (33) and (35), we can now calculate $\tilde{F}_{\pi^+}(n_1,n_2)$, which in turn are used in Eq. (36) to determine $\tilde{H}_{\pi^\pm}(n)$. The inversion to $H'_{\pi^\pm}(x)$ [and then trivially to $H_{\pi^\pm}(x)$] involves a method that has been discussed in Ref. [13] and is summarized in the Appendix. We show our results in Fig. 3. The solid lines are from our calculations with normalizations adjusted to fit the data [12], since the data are for the dimensionful $Ed^3\sigma/dp^3$ at fixed p_T while our model is for the dimensionless xdN/dx, integrated over all p_T. The shapes of the calculated inclusive distributions involve no adjustable parameters. Evidently, they agree very well with the x dependences of the data. We regard this result as evidence in support of the VRM.

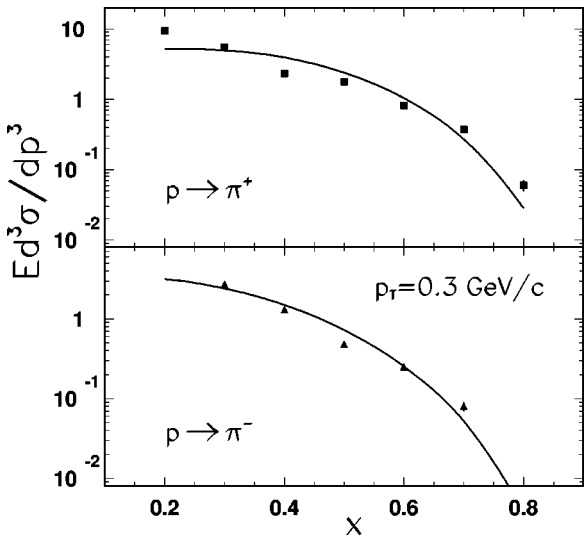

FIG. 3. Inclusive distributions of $p \to \pi^+$ and π^-. The data are from Ref. [12] at $P_L = 100$ GeV/c and $p_T = 0.3$ GeV/c.

IV. PION FRAGMENTATION: $\pi^+ \to \pi^-$

In this section we consider the nondiffractive inclusive distribution of $\pi^+ \to \pi^-$ in the fragmentation region of the pion beam. By charge conjugate invariance it should be the same as for $\pi^- \to \pi^+$, if there is no contamination by target fragmentation. Since there are no valence quarks of the projectile that end up in the produced pion, one naively would expect dN/dx to be strongly suppressed at high x. Yet experimental data [12] indicate that its x dependence is rather similar to that of $p \to \pi^+$, in which a u quark is shared between p and π^+. Thus simple fragmentation of a valence quark or diquark in a string model cannot account for this similarity. In the VRM because the valon distribution in the pion is different from the ones in the proton, with the former giving larger average momentum fraction of the valons than the latter, large-x π^- in π^+ can arise from the higher-momentum valons. In this section we show this behavior quantitatively.

For $\pi^+ \to \pi^-$ the invariant distribution $H_{\pi^+ \to \pi^-}(x)$ has the same formal expression as Eq. (29) except that F_π for p fragmentation is to be replaced by $F_{\pi^+ \to \pi^-}$. In Fig. 4 we show the schematic diagrams for $U\bar{D}$ valons going to $d\bar{u}$ quarks. The moments for $F_{\pi^+ \to \pi^-}$ can then be written down by inspection,

$$\tilde{F}_{\pi^+ \to \pi^-}(n_1,n_2) = \tilde{G}^{\pi}_{U\bar{D}}(n_1,n_2)[\tilde{L}'_f(n_1)\tilde{L}'_f(n_2) + \tilde{L}'_u(n_1)\tilde{L}'_u(n_2)] + [\tilde{G}^{\pi}_{U}(n_1) + \tilde{G}^{\pi}_{\bar{D}}(n_2)] \times \{\tilde{L}'_f(n_1,n_2)\tilde{L}_u(n_2)\}_{12}. \quad (47)$$

We note that $\bar{u}$ is favored in U, and d is favored in $\bar{D}$. Because we assume that the structure of valons is universal in all host hadrons, the enhanced sea of a valon in the pion is the same as that of a valon in the proton; thus $\tilde{L}'_{f,u}$ is the same as in the previous section.

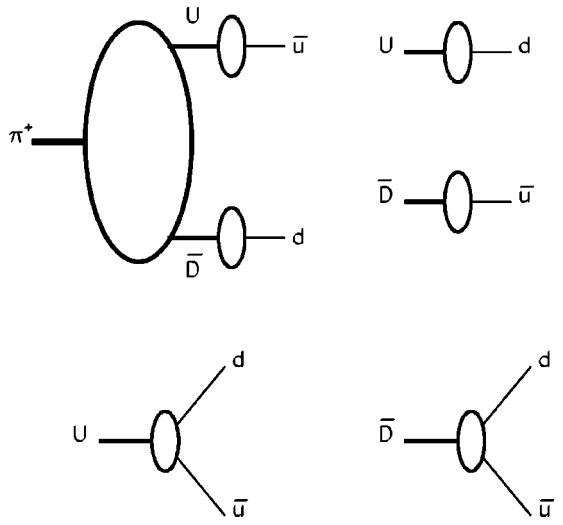

FIG. 4. Schematic diagrams in the VRM for $\pi^+ \to d\bar{u}$.

Since $G^{\pi}_{U\bar{D}}(y_1,y_2) = \delta(y_1+y_2-1)$ due to $\gamma = 0$ in Eq. (19), we have

$$\tilde{G}^{\pi}_{U\bar{D}}(n_1,n_2) = B(n_1,n_2), \quad (48)$$

$$\tilde{G}^{\pi}_{U,\bar{D}}(n_i) = 1/n_i. \quad (49)$$

The calculation of $\tilde{F}_{\pi^+ \to \pi^-}(n_1,n_2)$ is therefore straightforward. Using it in Eq. (36) yields $\tilde{H}_{\pi^+ \to \pi^-}(n)$, and by inversion we get $H_{\pi^+ \to \pi^-}(x)$.

The result is shown in Fig. 5 by the solid line. The dotted line is the fit of the data given by the experimental paper [12], where the $x \geq 0.6$ points are excluded in order to avoid contamination from resonance decay products. Our result agrees very well with the experimental parametrization of the

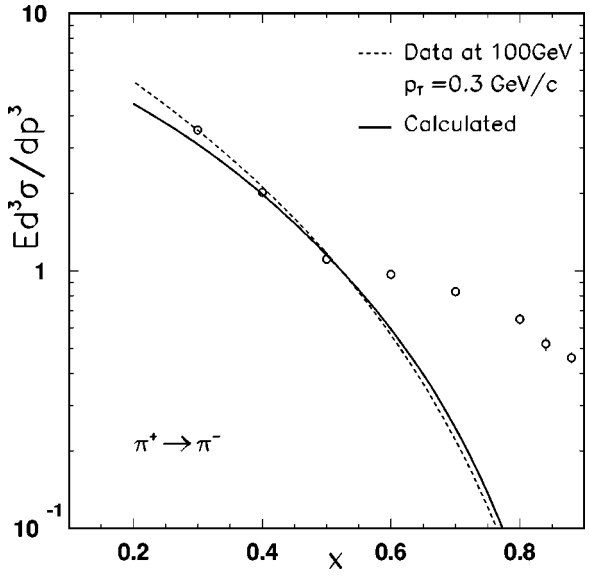

FIG. 5. Inclusive distributions of $\pi^+ \to \pi^-$. Data are from Ref. [12]. The dotted line is the experimental fit; the solid line is the theoretical result in the VRM.

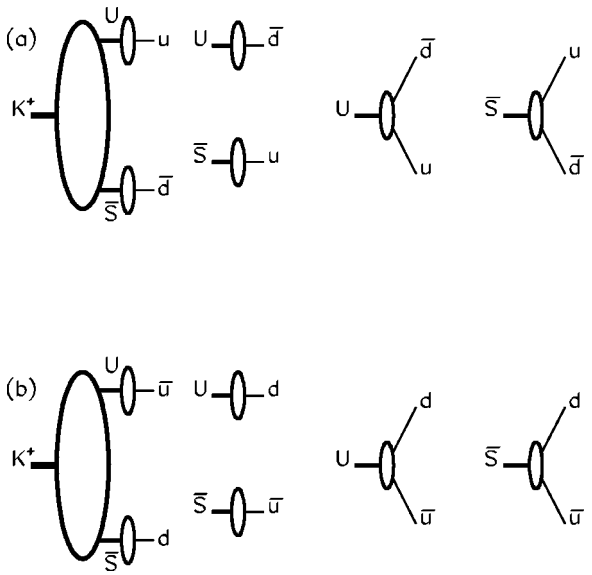

FIG. 6. Schematic diagrams in the VRM for (a) $K^+ \to u\bar{d}$ and (b) $K^+ \to d\bar{u}$.

data by $\sim(1-x)^m$ where $m=3.37\pm0.09$ for $p_T=0.3$ GeV/c at beam momentum 100 GeV/c.

The lack of $\tilde{K}$ in Eq. (47) compared to Eqs. (33) and (35), corresponding to no valence quarks, is compensated by the fact that $\tilde{G}^{\pi}_{UD}$ and $\tilde{G}^{\pi}_{U,D}$ in Eqs. (48) and (49) are not as damped at high n_i as $\tilde{G}^{p}_{UU}$, $\tilde{G}^{p}_{UD}$, and $\tilde{G}^{p}_{U,D}$ are in Eq. (37), (38), (9), and (10), respectively, for α and β being as big as in Eq. (5). That is, in π^+ we have harder valons and softer d and $\bar{u}$, while in p we have softer valons and harder u and $\bar{d}$.

The normalization of the calculated distribution in Fig. 5 is again adjusted to fit, since the data are for inclusive cross section at fixed p_T. Nevertheless, the agreement of the x dependence with data is the second piece of support one can infer for VRM.

V. KAON FRAGMENTATION: $K^+ \to \pi^{\pm}$

In Sec. II we have discussed the form of the valon distributions in a kaon with one undetermined parameter to be fixed. Now we consider kaon initiated reactions and determine that parameter by fitting the inclusive distribution of $K^+ \to \pi^{\pm}$.

From Eq. (23) we have

$$\tilde{G}^{K}_{U\bar{S}}(n_1,n_2)=B(n_1+a,n_2+b)/B(a+1,b+1), \quad (50)$$

$$\tilde{G}^{K}_{U}(n_1)=B(n_1+a,b+1)/B(a+1,b+1), \quad (51)$$

$$\tilde{G}^{K}_{\bar{S}}(n_2)=B(a+1,n_2+b)/B(a+1,b+1), \quad (52)$$

where a and b are constrained by Eq. (26). In Fig. 6 we show the schematic diagrams for (a) $K^+ \to \pi^+$ and (b) $K^+ \to \pi^-$. It then follows that:

$$\begin{aligned}\tilde{F}_{K^+\to\pi^+}(n_1,n_2)=\tilde{G}^{K}_{U\bar{S}}(n_1,n_2)&[\tilde{K}(n_1)\tilde{L}''_u(n_2)\\&+\tilde{L}'_u(n_1)\tilde{L}''_u(n_2)]+\tilde{G}^{K}_{U}(n_1)\\&\times\{\tilde{K}(n_1,n_2)\tilde{L}'_u(n_2)\}_{12}+\tilde{G}^{K}_{\bar{S}}(n_2)\\&\times\{\tilde{L}''_u(n_1,n_2)\tilde{L}''_u(n_2)\}_{12}, \quad (53)\end{aligned}$$

where $\tilde{L}''_u(n_2)$ is the moment of the enhanced, unfavored quark distribution in the $\bar{S}$ valon, and will be discussed below. Similarly, we have for $K^+ \to \pi^-$

$$\begin{aligned}\tilde{F}_{K^+\to\pi^-}(n_1,n_2)=\tilde{G}^{K}_{U\bar{S}}(n_1,n_2)&[\tilde{L}'_f(n_1)\tilde{L}''_u(n_2)\\&+\tilde{L}'_u(n_1)\tilde{L}''_u(n_2)]+\tilde{G}^{K}_{U}(n_1)\\&\times\{\tilde{L}'_u(n_1,n_2)\tilde{L}'_f(n_2)\}_{12}+\tilde{G}^{K}_{\bar{S}}(n_2)\\&\times\{\tilde{L}''_u(n_1,n_2)\tilde{L}''_u(n_2)\}_{12}. \quad (54)\end{aligned}$$

For gluon conversion in the $\bar{S}$ valon we again consider the saturation of the $u\bar{u}$ and $d\bar{d}$ sectors of the sea, but none in the $s\bar{s}$ sector because of the higher s-quark mass. Since the nonstrange sectors are both unfavored, the momentum carried by the sea is not the same as that in a nonstrange valon. Thus we write before gluon conversion

$$\tilde{K}_{NS}(2)+4\tilde{L}^{S}_{u}(2)+2\tilde{L}^{S}_{s}(2)+\tilde{L}^{S}_{g}(2)=1, \quad (55)$$

where $\tilde{L}^{S}_{i}(i=u,s,g)$ refer to the $\bar{S}$ valon. Equation (55) differs from Eq. (39) for a $\bar{D}$ valon only in that the favored sector $d\bar{d}$ is replaced by the unfavored sector $d\bar{d}$. It means that there is a redistribution of the momenta in the gluons and sea quarks, which, we assume, takes the simple form

$$\tilde{L}^{S}_{i}(2)=c\tilde{L}_i(2), \quad (56)$$

where c is a constant. After gluon conversion Eq. (55) becomes

$$\tilde{K}_{NS}(2)+4\tilde{L}''_u(2)+2\tilde{L}^{S}_{s}(2)=1. \quad (57)$$

If we define $\tilde{L}''_u(2)=f_s\tilde{L}^{S}_{s}(2)$, we obtain

$$f_s=1+\tilde{L}^{S}_{g}(2)/4\tilde{L}^{S}_{u}(2)=1+\tilde{L}_g(2)/4\tilde{L}_u(2). \quad (58)$$

Using as before $\tilde{L}_u(2)=e^{-3.07}$ and $\tilde{L}_g(2)=e^{-0.98}$, we get

$$f_s=3.02. \quad (59)$$

To determine $\tilde{L}''_u(2)$ in terms of $\tilde{L}_u(2)$ we need, in addition to f_s, the value of c in Eq. (56). It follows from Eqs. (39), (55), and (56) that

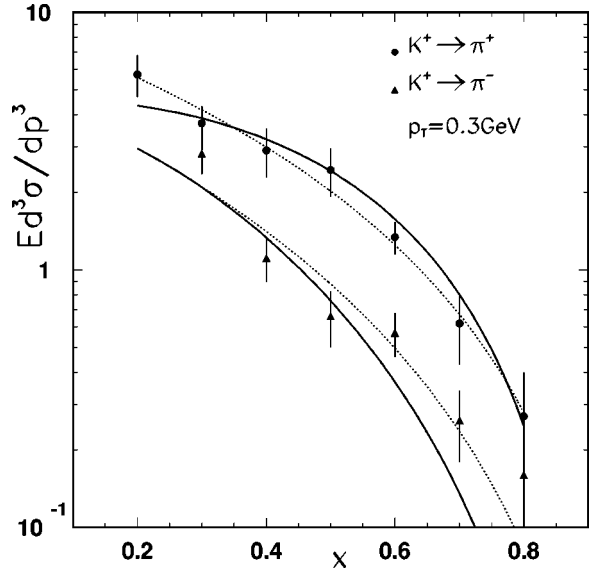

FIG. 7. Inclusive distributions of $K^+ \to \pi^+$ and $K^+ \to \pi^-$. The data are from Ref. [12] $P_L = 100$ GeV/c and $p_T = 0.3$ GeV/c. The dotted lines are the experimental fits; the solid lines are the theoretical results in the VRM.

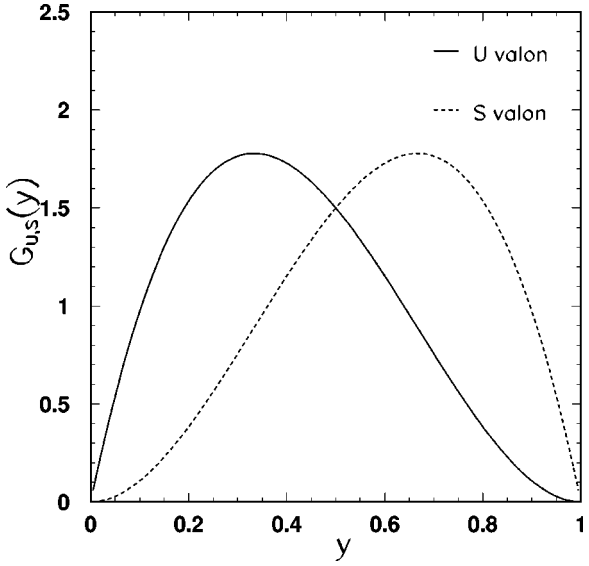

FIG. 8. The momentum-fraction distributions of the valons in a kaon: (a) U valon in solid lines and (b) $\bar{S}$ valon in dotted line.

$$c = 1 - \frac{2[\tilde{L}_u(2) - \tilde{L}_f(2)]}{4\tilde{L}_u(2) + 2\tilde{L}_s(2) + \tilde{L}_g(2)}. \tag{60}$$

Since $\tilde{L}_s(2) = e^{-4.21}$ from Table I, we get

$$c = 0.9 \tag{61}$$

and finally $\tilde{L}''_u(2) = f_s c \tilde{L}_u(2) = 2.72\tilde{L}_u(2)$. Again, extending this proportionality to all n_2, we have

$$\tilde{L}''_u(n_2) = 2.72\tilde{L}_u(n_2). \tag{62}$$

We now have all the quantities in Eqs. (52) and (54) to calculate $\tilde{F}_{K^+ \to \pi^\pm}(n_1, n_2)$.

There is one adjustable parameter in our calculation. It is a in Eq. (23), b being constrained by Eq. (26). After $\tilde{F}_{K^+ \to \pi^\pm}(n_1, n_2)$ are determined, we use a formula similar to Eq. (36), i.e.,

$$\tilde{H}'_{K^+ \to \pi^\pm}(n) = \sum_{[n_i]} \frac{n!}{n_1! n_2!} \tilde{F}_{K^+ \to \pi^\pm}(n_1 + 2, n_2 + 2), \tag{63}$$

to calculate $\tilde{H}'_{K^+ \to \pi^\pm}(n)$. Then by inversion to $H'_{K^+ \to \pi^\pm}(x)$ as before, we can finally obtain $H_{K^+ \to \pi^\pm}(x) = x^{-3}\tilde{H}'_{K^+ \to \pi^\pm}(x)$. We adjust a to fit the data, which are shown in Fig. 7 for $p_T = 0.3$ GeV/c. Again, because the data are for fixed p_T, we cannot predict the normalization, which is adjusted to fit. The best values of a and b are

$$a = 1.0, \quad b = 2.0. \tag{64}$$

The solid lines in Fig. 7 show the calculated results; the dotted lines are the experimental fits using the form $(1 - x)^m$. Although the fits are not perfect, they are acceptable in view of the large error bars in the data. What is noteworthy is that we used only one normalization factor for both π^+ and π^- production, and the calculated curves agree with the two sets of data in their relative normalizations. Thus the VRM has captured the essence of $\pi^\pm$ production in K^+ initiated reactions.

Since a and b are now known, we can exhibit the valon distributions in a kaon. In Fig. 8 we show $G_U^K(y)$ and $G_{\bar{S}}^K(y)$. Note how the strange valon has larger momentum fraction than the nonstrange valon, on the average. It is because of the harder $\bar{S}$ valon, though softer nonstrange quarks in it, that gives rise to the distributions $H_{K^+ \to \pi^\pm}(x)$ that are harder (decreasing more slowly with x) than either $\pi^+ \to \pi^-$ or even $p \to \pi^+$, which has a shared valence quark. This is a remarkable affirmation of the importance of the structure of the hadron in the determination of the inclusive distributions of its fragments.

VI. PION FRAGMENTATION: $\pi^+ \to K^\pm$

Since the valon distributions in the kaon have been determined in the previous section, we now know the recombination function for the formation of kaon. Thus the calculation of pion fragmentation into $K^\pm$ should be straightforward.

In Fig. 9 we show the diagrams for $\pi^+ \to K^\pm$. They are essentially the same as the ones in Fig. 6 for $K^+ \to \pi^\pm$, except for the replacement of $\bar{S}$ valon in the initial K^+ by $\bar{D}$ valon in the initial π^+, and the replacement of the appropriate nonstrange q and $\bar{q}$ quarks in $\pi^\pm$ by the s and $\bar{s}$ quarks in $K^\pm$. The corresponding equations are therefore similar to Eqs. (52) and (54),

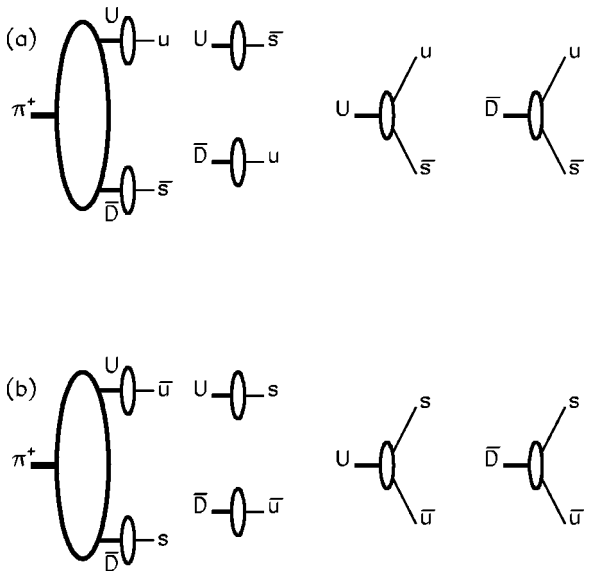

FIG. 9. Schematic diagrams in the VRM for (a) $\pi^+ \to u\bar{s}$ and (b) $\pi^+ \to s\bar{u}$.

$$\tilde{F}_{\pi^+\to K^+}(n_1,n_2) = \tilde{G}^{\pi}_{U\bar{D}}(n_1,n_2)[\tilde{K}(n_1)\tilde{L}_s(n_2) + \tilde{L}_s(n_1)\tilde{L}'_u(n_2)] + \tilde{G}^{\pi}_{U}(n_1) \times \{\tilde{K}(n_1,n_2)\tilde{L}_s(n_2)\}_{12} + \tilde{G}^{\pi}_{\bar{D}}(n_2) \times \{\tilde{L}'_u(n_1,n_2)\tilde{L}_s(n_2)\}_{12}, \quad (65)$$

$$\tilde{F}_{\pi^+\to K^-}(n_1,n_2) = \tilde{G}^{\pi}_{U\bar{D}}(n_1,n_2)[\tilde{L}'_f(n_1)\tilde{L}_s(n_2) + \tilde{L}_s(n_2)\tilde{L}'_u(n_1)] + \tilde{G}^{\pi}_{U}(n_1) \times \{\tilde{L}'_f(n_1,n_2)\tilde{L}_s(n_2)\}_{12} + \tilde{G}^{\pi}_{\bar{D}}(n_2) \times \{\tilde{L}'_u(n_1,n_2)\tilde{L}_s(n_2)\}_{12}. \quad (66)$$

Note that $\tilde{L}_s(n_i)$ is not enhanced because, as before, gluon conversion saturates the nonstrange sectors of the sea. The other moments are as given in Sec. IV.

Since the recombination function R_K is now different from R_π, the inclusive distribution for $K^\pm$ production is

$$x\frac{dN_K}{dx} = H_K(x) = \int \frac{dx_1}{x_1}\frac{dx_2}{x_2} F_{\pi\to K}(x_1,x_2) R_K(x_1,x_2,x) = g_K x^{-4} \int dx_1 dx_2 x_1 x_2^2 F_{\pi\to K}(x_1,x_2) \times \delta(x_1+x_2-x), \quad (67)$$

where Eqs. (28) and (64) have been used. If we define

$$H'_K(x) = x^6 H_K(x), \quad (68)$$

then the binomial expansion of $(x_1+x_2)^n$ leads us to the moments

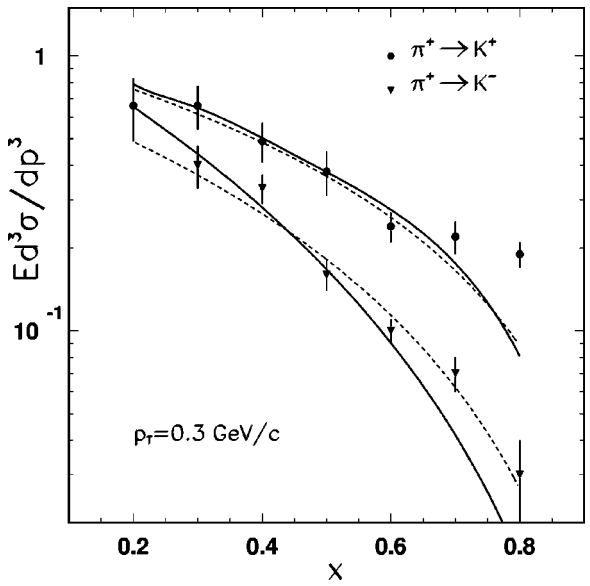

FIG. 10. Inclusive distributions of $\pi^+ \to K^+$, and (b) $\pi^+ \to K^-$. The data are from Ref. [12] $P_L = 100$ GeV/c and $p_T = 0.3$ GeV/c. The dotted lines are the experimental fits; the solid lines are the theoretical results in the VRM.

$$\tilde{H}'_K(n) = \int_0^1 dx x^{n-2} H'_K(x) = g_K \sum_{[n_i]} \frac{n!}{n_1! n_2!} \tilde{F}_{\pi\to K}(n_1+3, n_2+4), \quad (69)$$

similar, but not identical, to Eq. (36). In view of Eqs. (65) and (66), $\tilde{H}'_{K^\pm}(n)$ can now be calculated without any free parameters.

Using the same procedure as before to obtain $H_{K^\pm}(x)$, we can determine the inclusive distributions for $\pi^+ \to K^\pm$. In Fig. 10 we show our results compared to the data [12] at 100 GeV/c and $p_T = 0.3$ GeV/c. Again, the normalization is adjusted to fit, but only one normalization factor for both curves. The agreement between theory and experiment is very good, considering that no free parameter is used except for the overall normalization. The excess for $x > 0.6$ can be attributed to the decay of K^* whose K product would have higher x. The relative normalization of K^+ to K^- is well reproduced by VRM.

VII. CONCLUSION

We have considered the production of mesons in the fragmentation regions of incident proton and mesons in low-p_T collisions. The data on $p \to \pi^\pm$, $\pi^+ \to \pi^-$, $K^+ \to \pi^\pm$, and $\pi^+ \to K^\pm$ have all been satisfactorily reproduced by the calculated results in the VRM. There is essentially only one free parameter that is connected with the valon distribution in the kaon. All other parameters specifying the structure of the proton and pion have been determined independently by fit-

ting the data on hard processes. It is self-evident that by successfully reproducing the inclusive distributions of all the above reactions we have met the test of charge asymmetry in $\pi^+ p$ collisions.

Apart from the details of the VRM and of the data in the fragmentation region, the fundamental themes that this work has affirmed are that the hadron structures are important and that hadronization proceeds through recombination. The valon model effectively describes the hadron structure and the valon distributions provide the probability functions for recombination. It is conceivable that two valons may be regarded as a diquark whose fragmentation yields the produced mesons. Since the two valons are spatially distributed objects with nonvanishing relative momentum, to describe their fragmentation by a fragmentation function adapted from jet physics seems hard to justify. The VRM, on the other hand, is related more closely to the parton model and provides a natural *s*-channel description of the fragmentation process (from the point of view of the hadron) in terms of recombination (from the point of view of the quarks and antiquarks).

We have not considered the production of baryons in this paper. However, the nondiffractive production of nucleons in *pA* collisions has already been treated in the VRM [13]. The production of strange particles is worthy of further attention. Our consideration of $\pi^+ \to K^\pm$ is only a beginning, which shows that in hadronic collisions gluons do not convert to $s\bar{s}$ as effectively as to $u\bar{u}$ and $d\bar{d}$. That situation must change in going from hadronic to nuclear collisions due to Pauli blocking in the nonstrange sector. It seems that the VRM provides a natural framework in which to investigate the transition from strangeness suppression to strangeness enhancement.

ACKNOWLEDGMENTS

One of us (R.C.H.) is grateful to Professor A. Capella for stimulating discussions that have led to a challenge for us to show how well the recombination model works. This work was supported, in part, by the U.S. Department of Energy under Grant No. DE-FG03-96ER40972.

APPENDIX

We summarize here the method of inversion from the moments to the *x*-distribution function, originally proposed in Ref. [13]. Instead of making the inverse Mellin transform, which involves a complex contour, we exploit the orthogonality of the Legendre polynomials. First, we shift the variable to the interval $0 \leqslant x \leqslant 1$, and define

$$g_l(x) = P_l(2x-1) \tag{A1}$$

so that

$$\int_0^1 dx g_l(x) g_m(x) = \frac{1}{2l+1}\delta_{lm}. \tag{A2}$$

If we expand the distribution $H'(x)$ in terms of $g_l(x)$,

$$H'(x) = \sum_{l=0}^{\infty} (2l+1) h_l g_l(x), \tag{A3}$$

then the inverse is

$$h_l = \int_0^1 dx H'(x) g_l(x). \tag{A4}$$

These h_l can be expressed in terms of the moments $H'(n)$ if we express $g_l(x)$ as a power series in x,

$$g_l(x) = \sum_{i=0}^{l} a_l^i x^i, \tag{A5}$$

where a_l^i are known from the properties of $P_l(z)$. Thus from Eq. (A4) we have

$$h_l = \sum_{i=0}^{l} a_l^i \tilde{H}'(i+2), \tag{A6}$$

where $\tilde{H}'(n)$ is defined in Eq. (36). It is now clear that our theoretical results in $\tilde{H}'(n)$ can be transformed to $H'(x)$ through Eqs. (A3) and (A6) once we have the coefficients a_l^i. Furthermore, if $\tilde{H}'(n)$ becomes unimportant for $n > N$, then the sum in Eq. (A3) can terminate at N.

To determine a_l^i, we make use of the recursion formula

$$(l+1)P_{l+1}(z) = (2l+1)zP_l(z) - lP_{l-1}(z) \tag{A7}$$

to infer through Eqs. (A1) and (A5)

$$a_l^0 = -\frac{1}{l}[(2l-1)a_{l-1}^0 + (l-1)a_{l-2}^0], \tag{A8}$$

$$a_l^i = -\frac{1}{l}[(2l-1)(a_{l-1}^i - 2a_{l-1}^{i-1}) + (l-1)a_{l-2}^i], \tag{A9}$$

where $l \geqslant 2$, and $1 \leqslant i \leqslant l$. For $l < 2$, we have

$$a_0^0 = 1, \quad a_1^0 = -1, \quad a_1^1 = 2. \tag{A10}$$

With these we can generate all a_l^i, so h_l can be directly computed. The use of Eq. (A3) then yields $H'(x)$.

We have found that this method can give very accurate result in inverting $\tilde{H}'(n)$ to $H'(x)$ for N roughly between 8 and 10, depending on how rapidly $\tilde{H}'(n)$ decreases with n.

[1] *Partons in Soft-Hadronic Processes*, edited by R. T. Van de Walle (World Scientific, Singapore, 1981).
[2] K. Fiałkowski and W. Kittel, Rep. Prog. Phys. **46**, 1283 (1983).
[3] A. Capella, U. Sukhatme, C.-I. Tan, and J. Tran Thanh Van, Phys. Rep. **236**, 225 (1994).
[4] B. Andersson, G. Gustafson, and C. Peterson, Phys. Lett. **69B**, 221 (1977); **71B**, 337 (1977); B. Andersson, G. Gustafson, G. Ingelman, and T. Sjöstrand, Phys. Rep. **97**, 33 (1983).

[5] K.P. Das and R.C. Hwa, Phys. Lett. **68B**, 459 (1977).
[6] R.C. Hwa, Phys. Rev. D **22**, 1593 (1980).
[7] H.L. Lai *et al.*, CTEQ Collaboration, Phys. Rev. D **51**, 4763 (1995).
[8] R.C. Hwa, Phys. Rev. D **22**, 759 (1980); R.C. Hwa and M.S. Zahir, *ibid.* **23**, 2539 (1981).
[9] R.C. Hwa and C.B. Yang, Phys. Rev. C **66**, 025204 (2002), preceding paper.
[10] W. Ochs, Nucl. Phys. **B118**, 397 (1977).
[11] Figure 4.8 in Ref. [3].
[12] A.E. Brenner *et al.*, Phys. Rev. D **26**, 1497 (1982).
[13] R.C. Hwa and C.B. Yang, Phys. Rev. C **65**, 034905 (2002).
[14] CTEQ4LQ, http://zebu.uoregon.edu/~parton/partongraph.html
[15] P.J. Sutton, A.D. Martin, R.G. Roberts, and W.J. Stirling, Phys. Rev. D **45**, 2349 (1992).